CHAPTER TWO

Imaging White Adipose Tissue with Confocal Microscopy

Gabriel Martinez-Santibañez[*], **Kae Won Cho**[†], **Carey N. Lumeng**[†,1]
[*]Cellular and Molecular Biology Program, University of Michigan, Ann Arbor, Michigan, USA
[†]Department of Pediatrics and Communicable Diseases, University of Michigan Medical School, Ann Arbor, Michigan, USA
[1]Corresponding author: e-mail address: clumeng@umich.edu

Contents

Abstract

Adipose tissue is composed of a variety of cell types that include mature adipocytes, endothelial cells, fibroblasts, adipocyte progenitors, and a range of inflammatory leukocytes. These cells work in concert to promote nutrient storage in adipose tissue depots and vary widely based on location. In addition, overnutrition and obesity impart significant changes in the architecture of adipose tissue that are strongly associated with

Methods in Enzymology, Volume 537
ISSN 0076-6879
http://dx.doi.org/10.1016/B978-0-12-411619-1.00002-1

metabolic dysfunction. Recent studies have called attention to the importance of adipose tissue microenvironments in regulating adipocyte function and therefore require techniques that preserve cellular interactions and permit detailed analysis of three-dimensional structures in fat. This chapter summarizes our experience with the use of laser scanning confocal microscopy for imaging adipose tissue in rodents.

1. INTRODUCTION

Adipose tissue is comprised of a vast range of cellular and noncellular components. By volume, adipocytes are the most prominent cell within a given white fat depot. However, by cell number, it is likely that mature adipocytes are in the minority due to the presence of a large network of supporting cells (Granneman, 2008). These include cells that comprise an extensive vascular system in fat, including fibroblasts, preadipocytes, and cells with mesenchymal and hematopoietic stem cell capacity (Crandall, Hausman, & Kral, 1997; Nishimura et al., 2007; Zuk et al., 2002). Obesity research has called significant attention to the presence of a wide range of inflammatory leukocytes and lymphocytes in fat that change with obesity. These include myeloid cells (macrophages, neutrophils, etc.), lymphocytes (T cells, B cells), eosinophils, mast cells, and NK cells (Lee, Goldfine, Benoist, Shoelson, & Mathis, 2009; Nagasaki, Eto, Yamashita, Ohsugi, & Otsu, 2009; Nishimura et al., 2009; Ohmura et al., 2010). Quantitation and localization of these cells is a critical part of understanding the link between obesity and inflammation. A significant need to understand this association has spurred the development of techniques that permit a detailed examination of the diverse components and architecture of adipose tissue.

Traditional histologic techniques for adipose tissue analysis have included electron microscopy (transmission and scanning) and freeze fracturing. Many laboratories analyze adipose tissue with light microscopy (LM) techniques such as immunohistochemistry and *in situ* hybridization (Cinti, Zingaretti, Cancello, Ceresi, & Ferrara, 2001). However, because of the high lipid content in fat, sectioning of frozen or paraffin-embedded samples is often inconsistent and can distort adipose tissue architecture. This can lead to biased assessments of adipocyte size. More importantly, this limits our capacity to appreciate the diversity of nonadipocyte cell types in fat, and limits our ability to observe their cell–cell interactions. For those reasons, we and others have developed techniques that permit the imaging of whole-mount tissue samples in a way that maintains native architecture

(Cho et al., 2007; Lumeng, DelProposto, Westcott, & Saltiel, 2008). Here, we present a detailed description of the adipose tissue structures that can be imaged with confocal microscopy in rodents, along with detailed protocols.

1.1. Adipocyte morphology

The mature white adipocyte is primarily composed of a single large lipid droplet that is ~100 μm in diameter in mice (Suzuki, Shinohara, Ohsaki, & Fujimoto, 2011). Nuclear and other subcellular components are localized within a very thin cytoplasmic layer that lines the lipid droplet and forms the ghost-like remnant of the adipocyte seen in traditional paraffin-embedded sections. Immature adipocytes contain multiple small lipid droplets and are described as having a "multilocular" appearance. As the adipocyte matures, these lipid droplets fuse and form the round "unilocular" droplet. The fluorescent stains BODIPY and Nile Red are lipid-soluble compounds that help visualize lipid aggregation (Table 2.1).

The adipocyte plasma membrane contains numerous receptors (e.g., insulin receptors) involved in cell signaling that can regulate lipid uptake and fatty acid trafficking. Of these, Caveolin-1 is enriched in the plasma membrane and is commonly found in lipid rafts (Jasmin, Frank, & Lisanti, 2012). Because Caveolin-1 is abundant on the cell surface, it provides an excellent target for staining and imaging the plasma membrane of

Table 2.1 Adipocyte physiology and vascular structures

Target	Antibody or stain	Dilution	With saponin
Capillary and vasculature	Isolectin GS IB_4 (Invitrogen; Cat. # varies by conj. fluorochrome)	1:500	–
Lipid	BODIPY 493/503 (Invitrogen)	0.25 μg/mL	–
	Nile Red (Sigma N3013)	0.26 mg/mL	
Nuclei	DAPI	1 μg/mL	–
Cell membranes	Caveolin-1 (BD Biosciences 610060)	1 μg/mL	+
Lipid droplet surface	Perilipin (abcam ab61682)	2 μg/mL	+

Note: A "+" sign denotes that 0.1% saponin is required for membrane permeabilization due to intracellular localization of antigen.

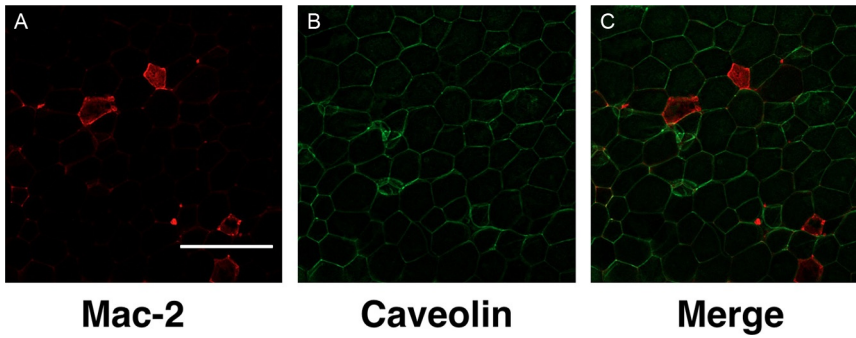

Figure 2.1 Crown-like structures in white adipose tissue. Gonadal fat pads from a high fat diet fed C57Bl/6 mouse were fixed, isolated, and stained as above. Macrophages stain Mac-2 in red (A), Caveolin-1 plasma membrane in green (B), and images were merged (C). Scale bar = 350 μm.

adipocytes. Lipid droplets are surrounded by PAT proteins (i.e., perilipin, ADRP, TIP47), which regulate both storage and release of lipids. Perilipin is a useful marker of lipid droplet structures in white fat. Stimulation by adrenergic agonists changes the conformation of perilipin, which allows access of lipases, like hormone-sensitive lipase, to the lipid droplet. This results in the mobilization of triglycerides (Greenberg et al., 1991). Perilipin is also useful for identifying dead or dying adipocytes where loss of perilipin staining is noted (Feng et al., 2011). For reagents useful in visualizing these structures, refer to Table 2.1.

1.2. Adipose tissue macrophages and crown-like structures

The death of adipocytes results in marked remodeling of the adipose tissue microenvironment. H&E sections and immunohistochemistry studies have revealed that areas with adipocyte death create regions called crown-like structures (CLSs) that are described as accumulations of proinflammatory macrophages and extracellular matrix material (Cinti, 2005; Spencer et al., 2010) (Fig. 2.1). Dying adipocytes leave behind Perilipin-negative lipid droplets that also lack Caveolin-1 staining (Feng et al., 2011; Lumeng et al., 2008; Lumeng, Deyoung, Bodzin, & Saltiel, 2007). CLSs are a hallmark of adipose tissue inflammation and fibrosis in human and rodent adipose tissue.

A major cellular component of adipose tissue and CLSs is a population of adipose tissue macrophages (ATMs). Total ATMs can be detected in adipose tissue using a variety of macrophage-specific surface stains such as Mac-2 and F4/80 (Table 2.2). An example of how CLSs can be visualized is by using a

Table 2.2 Adipose tissue macrophage and crown-like structure stains

Target	Antibody	Dilution
Total ATMs	F4/80 (abcam ab6640)	1:300
	Galectin-3 (Mac-2) (eBioscience 14-5301-85)	1:200
M1 ATMs	CD11c (abD Serotech MCA1369)	1:200
M2 ATMs	MGL-1 (abcam ab15635)	1:300
Capillary and vasculature	Isolectin GS IB_4 (Invitrogen; cat. no. varies by conj. fluorochrome)	1:500

combination of macrophage stain and perilipin stain, where Mac-2 and/or F4/80 will reveal a circular organization of macrophages that is void of perilipin stain. Resident $CD11c^{-}/MGL\text{-}1^{+}$ M2 ATMs are seen in interstitial spaces between adipocytes and have morphologic characteristics that are distinct from $CD11c^{+}$ ATMs (Lumeng, Bodzin, & Saltiel, 2007; Xu et al., 2003). In contrast, $CD11c^{+}$ "classically activated" M1 ATMs are rare in lean mice, but are abundant in obese mice. These are enriched in CLS and are frequently found to contain triglyceride-laden lipid droplets. Resident ATMs lack lipid accumulation and are enriched for markers of M2 polarization such as CD206 and CD301/MGL-1. In addition to ATMs, CLS have been shown to be sites of accumulation of numerous other lymphocytes and leukocytes that include T cells (adipose tissue T cells, or ATTs), B cells, mast cells, and eosinophils (Nishimura et al., 2009; Ohmura et al., 2010; Tsui, Wu, Davidson, Alonso, & Leong, 2011). The trafficking of these cells to fat, and the mechanism by which they are enriched in CLSs, is still unclear.

1.3. Milky spots and fat-associated lymphoid clusters

Hypercellular clusters are known to reside on the surface of numerous adipose tissue depots. Milky spots (MSs) are found primarily in omental adipose tissue depots and are composed of macrophages and B and T lymphocytes (Fig. 2.2A–C). They have been shown to participate in the clearing of debris from the peritoneum and may play a role in adaptive immunity (Rangel-Moreno et al., 2009). Fat-associated lymphoid clusters (FALCs) have recently been described in mesenteric fat, as well as in gonadal fat depots in mice (Moro et al., 2010; Morris et al., 2013) (Fig. 2.2D–G). These contain a unique population of $Lin^{-}Kit^{+}Sca1^{+}$ innate lymphocytes. If FALC are identical or related to milky spots is not clear, but they both appear to participate in phagocytosis and immune surveillance in several contexts. While

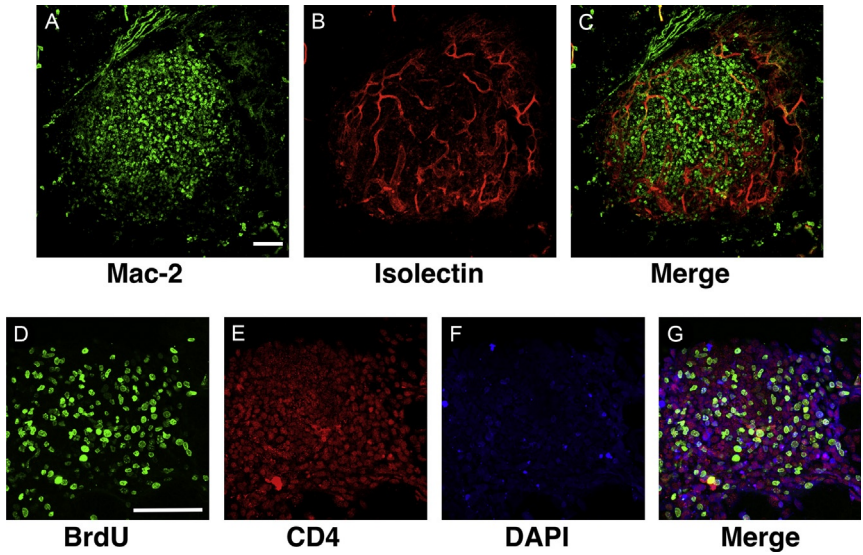

Figure 2.2 Milky spots and FALCS in adipose tissue. Omental fat pads from a C57Bl/6 mouse was fixed and stained and surface imaged to identify milky spots on the fat pad surface. Macrophages (Mac-2) are shown in green (A) and vasculature (isolectin) shown in red (B) with merged image (C). Gonadal fat pads were stained and imaged for surface collections of monocytes to identify FALCS. Proliferating cells are stained for BrdU in green (D), $CD4^+$ T cells are shown in red (E), nuclei are stained with DAPI in blue (F), and all three channels shown merged (G). Scale bar = 100 μm.

they appear to resemble lymph nodes, there is little evidence of associated lymphatic vessels.

The sizes of these uncapsulated structures range between 100 and 500 μm in diameter and are in direct contact with adipocytes (Rangel-Moreno et al., 2009). They appear to expand in concert with obesity, adipose tissue inflammation, and also in response to aging (Lumeng et al., 2011). The localization of such structures is a challenge in tissue sections as they are relatively rare on the surface of fat. However, whole-mount techniques facilitate the localization and characterization of FALCs and MSs. To image these structures, combination stains for nuclei (DAPI), T cells (CD4), and macrophages (F4/80) can be implemented (Table 2.2).

1.4. Capillaries and blood vessels

Adipose tissue contains an extensive vascular network that participates in the transport of nutrients and leukocytes in and out of fat. Many of the vascular

structures are tightly associated with CLS and FALCSs and are believed to facilitate cellular trafficking of leukocytes and lymphocytes (Nishimura et al., 2008). The formation of the primitive fat organ is dependent on the development of an extensive vascular bed (Crandall et al., 1997). Groups have found that the expansion of vascular networks occurs in concert, and even precedes adipogenesis (Han et al., 2011; Hausman & Richardson, 1983; Kimura, Ozeki, Inamoto, & Tabata, 2002). Adipose tissue growth, referring to both the expansion of number (hyperplasia) and size (hypertrophy), is tightly linked with angiogenesis. It has been demonstrated that limiting angiogenesis can also block adipogenesis (Brakenhielm et al., 2004; Liu & Meydani, 2003). In parallel with this idea, proangiogenic therapies can promote adipogenesis (Tabata et al., 2000). A general stain for adipose tissue vasculature is isolectin, which binds tightly to the surface of vascular endothelial cells (Cho et al., 2007; Nishimura et al., 2008) (Fig. 2.3).

1.5. Advantages of confocal imaging

The features in adipose tissue mentioned are complex, three-dimensional structures, thus the limitations of standard LM techniques are apparent. Furthermore, limiting sampling of fat to cross-sections will underrepresent structures such as FALCs and will not fully capture the three-dimensional tortuous route of many adipose tissue blood vessels. In addition, due to the high lipid content of fat, LM often results in significant auto-fluorescence, which is further promoted by light diffraction. The amount of auto-fluorescence can be determined simply by viewing a specimen that is unstained. Often the resolution of images taken with traditional microscopes is compromised because of the fluorescence signals that may arise

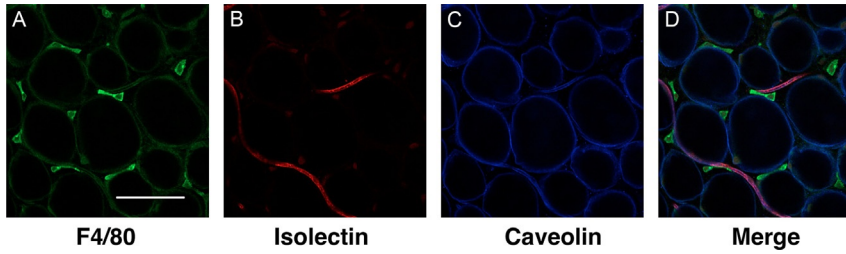

Figure 2.3 Adipose tissue vasculature. Gonadal fat pads from C57Bl/6 mice fed a chow diet. F4/80^{+} macrophages are stained in green (A), vasculature (isolectin) in red (B), Caveolin-1 denotes the adipocyte plasma membrane in blue (C), images merged in (D). Scale bar = 100 μm.

from other optical layers that are not within the plane of focus. Groups have attempted to alleviate this issue by cryosectioning methods and by flattening tissue fragments (Paddock & Eliceiri, 2014). However, such methods can significantly disturb the unique architecture of adipose tissue and may lead to highly variable results.

Laser scanning confocal imaging is an imaging technique that can address many of the limitations of traditional fluorescence microscopy. Because confocal imaging allows for visualizing a very narrow plane of focus, much of the interference that results from auto-fluorescence and out-of-focus blur can be removed. With proper fixation techniques and appropriate staining procedures whole-mount samples of adipose tissue can be imaged with confocal microscopy much more rapidly than with conventional LM techniques. Other advantages of confocal microscopy and its sophisticated optics include the use of specific excitation wavelengths, as well as the ability to employ detectors that exclude auto-fluorescence from other emission spectra. This feature comes into play when there is cross-fluorochrome excitation in neighboring light channels. In addition, *z*-stack series of images can be easily combined to assemble three-dimensional reconstruction of many of the unique structures within adipose tissue.

2. MATERIALS FOR IMAGING ADIPOSE TISSUE

2.1. Reagents and buffers

16% paraformaldehyde (PFA) 16% EM Grade (Electron Microscopy Sciences, Hatfield, PA; Cat. # 15710)
Phosphate-buffered saline (PBS), pH 7.4 (GIBCO Invitrogen, Carlsbad, CA; Cat. # 10010-023)
Bovine serum albumin (BSA) (Sigma-Aldrich, St. Louis, MO; Cat. # A7030)
Saponin (Sigma-Aldrich, St. Louis, MO; Cat. # 47036)
Glycerol (Sigma-Aldrich, St. Louis, MO; Cat. # G5516)
Tris base (Tris (Hydroxymethyl)Aminomethane) (EMD, Darmstadt, Germany; Cat. # 9230)
Fixing buffer: 1% PFA in PBS, pH 7.4 (v/v)
Blocking buffer: 5% BSA in PBS, pH 7.4 (w/v)
Intracellular stain buffer: 5% BSA in PBS, pH 7.4 (w/v) + 0.1% saponin
Intracellular stain wash buffer: PBS, pH 7.4 + 0.1% saponin
Buffered glycerol solution (optional)—for use as imaging stabilization agent 90% glycerol in 0.1 *M* Tris–HCl pH 9.0

2.2. Antibodies and suggested concentrations

See Tables 2.1-2.3 for antibody suppliers and suggested working concentrations.

2.3. Nuclear and lipid stains

BODIPY (4,4-difluoro-1,3,5,7,8-pentamethyl-4-bora-3*a*,4*a*-diaza-*s*-indacene) (Molecular Probes, Invitrogen, Carlsbad, CA; Cat. # D3922)
DAPI (40,6-diamidino-2-phenylindole dihydrochloride; Sigma-Aldrich, St. Louis, MO; Cat. # D9542)
Nile Red (Sigma-Aldrich, St. Louis, MO; Cat. # N3013)

2.4. Slides and equipment

Lab-Tek II Chambered #1.5 German borosilicate cover glass system (Nunc, Rochester, NY; Cat. # 155360)
2 mL cylindrical microcentrifuge tubes
Rotating/rocking platform
Inverted laser scanning confocal microscope— Olympus FluoView 500 is routinely employed in our lab but other brands and models are appropriate

3. METHODS

In order to best preserve structure and cellular components within adipose tissue and eliminate background fluorescence, perfusion fixation is recommended. Lower concentrations of fixative are typically employed to minimize auto-fluorescence. In addition, a gentle postfixation is beneficial immediately after tissue is removed. All buffers should be used at room temperature unless stated otherwise.

This protocol is routinely applied for confocal imaging of mouse adipose tissue from different depots. Similar protocols are possible in rats or other experimental animal models with alterations in the staining antibodies. The use of similar techniques in human adipose tissue samples may also be possible with some adaptation, but this has not been extensively tested.

3.1. Perfusion, collection, and fixation of white adipose tissues

1. Euthanize animals via cervical dislocation or CO_2 asphyxiation and perfuse via slow intracardiac injection with 10 mL of fresh fixing buffer (1% PFA in PBS, pH 7.4 (v/v), see Section 2.1) over 2–3 min. Injection can be via manual or pump through the left ventricle. Removal of the right atrium will facilitate removal of blood and clearance of fixative.

2. Excise white adipose tissue depots (i.e., epididymal, peri-renal and retroperitoneal, inguinal, omental). Tissues may be subdivided into 0.5–1 cm^3 sized pieces or left intact.
3. Incubate in 5–10 mL of fixing buffer for 30 min at room temperature with gentle rocking on a rotating platform. Make sure the tissue is completely submerged in fixation buffer. Longer fixation may increase auto-fluorescence.
4. Rinse away the fixing buffer with three, 10-min washes with PBS, pH 7.4, under gentle rocking at room temperature. Tissues may be stored at 4 °C in PBS, pH 7.4, for up to 2 weeks.

3.2. Blocking

To prevent fluorochrome-conjugated antibodies from nonspecific binding, a blocking step is suggested. The addition of a detergent during the blocking step is required for the detection of intracellular antigens (see Section 2.1).

5. Cut a piece from the fixed adipose tissue for staining. Typically this is 0.5–0.75 cm^3. Subsequent incubations are performed in 2 mL cylindrical microcentrifuge tubes.
6. Perform a 30-min block with 1 mL of blocking buffer (5% BSA in PBS, pH 7.4 (w/v)) with gentle rocking at room temperature. For staining intracellular antigens, perform this step with intracellular stain buffer.

3.3. Primary antibody incubation

7. Using blocking buffer (or intracellular stain blocking buffer if appropriate), prepare the primary antibody cocktail. Using a 2 mL microcentrifuge tube, 300 μL volume is typically sufficient to fully submerge one piece of tissue in antibody solution and allow for efficient mixing. (See Tables 2.1–2.3 for suggested staining targets and staining conditions.)

Table 2.3 Milky spot and FALC stains

Target	Antibody or stain	Dilution
CD4 T cells	CD4 (AbBiotech 250592)	1:200
Total ATMs	F4/80 (abcam ab6640)	1:200
Capillary and vasculature	Isolectin GS IB_4	1:500
Nuclei	DAPI	1 μg/mL

Note: Useful controls to include are: (1) unstained tissue to observe autofluorescence and (2) tissue stained with secondary antibody only to evaluate for any nonspecific staining.

8. Incubate tissues in primary antibody cocktail for 1 h at room temperature (or overnight at 4 °C) with gentle rocking. Antibody cocktail can be saved and reused at least two more times if stored at 4 °C for up to 4 weeks.
9. Perform three washes with gentle rocking, 10 min per wash, with PBS, pH 70.4 (or intracellular wash buffer if appropriate).

3.4. Secondary antibody incubation

10. Prepare fresh secondary antibody cocktail in 300 μL of antibody staining buffer (or use intracellular stain buffer) and incubate with gentle rocking for 1 h, covered, at room temperature.

Note: Titration may be necessary depending on the antibody source. Our laboratory typically uses AlexaFluor conjugated secondary antibodies (Molecular Probes by Life Technologies) at a dilution of 1:250 for a final concentration of 8 μg/mL.

If imaging vasculature structures, add the anti-isolectin antibody to the secondary antibody cocktail, refer to Table 2.1 for recommended concentrations.

11. Repeat step 9.
12. Tissues are ready for imaging. They can be stored, shielded from light, at 4 °C in PBS, pH 7.4, for 1–2 weeks. Continue to next step to stain lipid and nuclei.

3.5. Antibody-independent staining of nuclei and lipids

BODIPY (green channel), Nile Red (red channel), and DAPI (Ultraviolet or blue channel) stains can be performed independent of antibody-based stains. It is suggested that staining of lipids and nuclei be performed after antibody-based staining to prevent saturation of chemical-based fluorescence. Short incubations are recommended.

13. Prepare staining reagents in 5% BSA in PBS using suggested concentrations in Table 2.1.
14. Incubate tissues in lipid/nuclei staining cocktail for 20 min.
15. Perform three washes with gentle rocking, 10 min per wash, with PBS.
16. Tissues are ready for imaging or can be stored, shielded from light, in PBS at 4 °C in PBS for about 1–2 weeks.

3.6. Imaging and 3D reconstructions

Imaging of the stained tissue will take place on an inverted laser scanning confocal microscope. The tissue is placed atop confocal imaging optimized #1.5 borosilicate glass chamber slide. A small drop of PBS, pH 7.4 should be placed atop the piece of tissue to prevent drying. Alternatively, a glycerol-based stabilizing agent can be used (buffered glycerol solution) although storage of the fat samples after imaging can be difficult in this media.

Imaging capture will vary between experiment and system. We have been successful staining appropriately fixed samples with up to four laser lines (405, 488, 568, and 647 nm). Emission must be collected through the appropriate narrow band-pass filters by the confocal microscope. Adjustments for PMT, gain, and black levels vary and should be optimized per staining condition. If auto-fluorescence is an issue, it is possible to digitally remove it via image subtraction (Stockert, Villanueva, Cristóbal, & Cañete, 2009). Finally, assembly of three-dimensional reconstructions is accomplished by taking *z*-stack images using software-determined levels along the vertical axis.

4. SUMMARY

The protocols and images captured above provide a new depth of insight into the architecture and cell–cell interactions in adipose tissue with better resolution than LM techniques. While limited to static measurements, it is possible to use similar imaging modalities to evaluate dynamic leukocyte trafficking events into adipose tissue (Nishimura et al., 2008). We hope that these protocols provide a starting point for many researchers to explore and identify novel markers for use in adipose tissue imaging that can expand our knowledge of this dynamic organ.

ACKNOWLEDGMENTS

This work was supported by NIH Grants DK-090262 and DK-092873. This work used services at the University of Michigan NORC supported by NIH Grant DK-089503 and the Michigan Diabetes Research and Training Center funded by P60-DK-020572 from the National Institute of Diabetes and Digestive and Kidney Diseases. Special thanks to the Morphology and Image Analysis Core for training and equipment use.

REFERENCES

Brakenhielm, E., Cao, R., Gao, B., Angelin, B., Cannon, B., Parini, P., et al. (2004). Angiogenesis inhibitor, TNP-470, prevents diet-induced and genetic obesity in mice. *Circulation Research*, *94*(12), 1579–1588.

Cho, C. H., Jun Koh, Y., Han, J., Sung, H. K., Jong Lee, H., Morisada, T., et al. (2007). Angiogenic role of LYVE-1-positive macrophages in adipose tissue. *Circulation Research*, *100*(4), e47–e57.

Cinti, S. (2005). Adipocyte death defines macrophage localization and function in adipose tissue of obese mice and humans. *Journal of Lipid Research*, *46*(11), 2347–2355.

Cinti, S., Zingaretti, M. C., Cancello, R., Ceresi, E., & Ferrara, P. (2001). Morphologic techniques for the study of brown adipose tissue and white adipose tissue. *Methods in Molecular Biology (Clifton, NJ)*, *155*, 21–51.

Crandall, D. L., Hausman, G. J., & Kral, J. G. (1997). A review of the microcirculation of adipose tissue: Anatomic, metabolic, and angiogenic perspectives. *Microcirculation*, *4*(2), 211–232.

Feng, D. D., Tang, Y. Y., Kwon, H. H., Zong, H. H., Hawkins, M. M., Kitsis, R. N. R., et al. (2011). High-fat diet-induced adipocyte cell death occurs through a cyclophilin D intrinsic signaling pathway independent of adipose tissue inflammation. *Diabetes*, *60*(8), 2134–2143.

Granneman, J. G. (2008). Delivery of DNA into adipocytes within adipose tissue. *Methods in Molecular Biology (Clifton, NJ)*, *423*, 191–195.

Greenberg, A. S., Egan, J. J., Wek, S. A., Garty, N. B., Blanchette-Mackie, E. J., & Londos, C. (1991). Perilipin, a major hormonally regulated adipocyte-specific phosphoprotein associated with the periphery of lipid storage droplets. *Journal of Biological Chemistry*, *266*(17), 11341–11346.

Han, J., Lee, J.-E., Jin, J., Lim, J. S., Oh, N., Kim, K., et al. (2011). The spatiotemporal development of adipose tissue. *Development*, *138*(22), 5027–5037.

Hausman, G. J. G., & Richardson, R. L. R. (1983). Cellular and vascular development in immature rat adipose tissue. *Journal of Lipid Research*, *24*(5), 522–532.

Jasmin, J.-F., Frank, P. G., & Lisanti, M. P. (2012). *Caveolins and caveolae*. New York, NY: Springer.

Kimura, Y. Y., Ozeki, M. M., Inamoto, T. T., & Tabata, Y. Y. (2002). Time course of de novo adipogenesis in matrigel by gelatin microspheres incorporating basic fibroblast growth factor. *Tissue Engineering (United States)*, *8*(4), 603–613.

Lee, J., Goldfine, A. B., Benoist, C., Shoelson, S., & Mathis, D. (2009). Lean, but not obese, fat is enriched for a unique population of regulatory T cells that affect metabolic parameters. *Nature Medicine*, *15*(8), 930–939.

Liu, L., & Meydani, M. (2003). Angiogenesis inhibitors may regulate adiposity. *Nutrition Reviews*, *61*(11), 384–387.

Lumeng, C. N., Bodzin, J. L., & Saltiel, A. R. (2007). Obesity induces a phenotypic switch in adipose tissue macrophage polarization. *Journal of Clinical Investigation*, *117*, 175–184.

Lumeng, C. N., DelProposto, J. B., Westcott, D. J., & Saltiel, A. R. (2008). Phenotypic switching of adipose tissue macrophages with obesity is generated by spatiotemporal differences in macrophage subtypes. *Diabetes*, *57*(12), 3239–3246.

Lumeng, C. N., Deyoung, S. M., Bodzin, J. L., & Saltiel, A. R. (2007). Increased inflammatory properties of adipose tissue macrophages recruited during diet-induced obesity. *Diabetes*, *56*(1), 16–23.

Lumeng, C. N., Liu, J., Geletka, L., Delaney, C., Delproposto, J., Desai, A., et al. (2011). Aging is associated with an increase in T cells and inflammatory macrophages in visceral adipose tissue. *The Journal of Immunology*, *187*(12), 6208–6216.

Moro, K., Yamada, T., Tanabe, M., Takeuchi, T., Ikawa, T., Kawamoto, H., et al. (2010). Innate production of T(H)2 cytokines by adipose tissue-associated c-Kit(+)Sca-1(+) lymphoid cells. *Nature*, *463*(7280), 540–544.

Morris, D. L., Cho, K. W., Delproposto, J. L., Oatmen, K. E., Geletka, L. M., Martinez-Santibanez, G., et al. (2013). Adipose tissue macrophages function as antigen presenting cells and regulate adipose tissue CD4+ T cells in mice. *Diabetes*, *62*(8), 2762–2772.

Nagasaki, M., Eto, K., Yamashita, H., Ohsugi, M., & Otsu, M. (2009). CD8+ effector T cells contribute to macrophage recruitment and adipose tissue inflammation in obesity. *Nature Medicine*, *15*, 914–920.

Nishimura, S., Manabe, I., Nagasaki, M., Eto, K., Yamashita, H., Ohsugi, M., et al. (2009). CD8+ effector T cells contribute to macrophage recruitment and adipose tissue inflammation in obesity. *Nature Medicine*, *15*(8), 914–920.

Nishimura, S., Manabe, I., Nagasaki, M., Hosoya, Y., Yamashita, H., Fujita, H., et al. (2007). Adipogenesis in obesity requires close interplay between differentiating adipocytes, stromal cells, and blood vessels. *Diabetes*, *56*(6), 1517–1526.

Nishimura, S. S., Manabe, I. I., Nagasaki, M. M., Seo, K. K., Yamashita, H. H., Hosoya, Y. Y., et al. (2008). In vivo imaging in mice reveals local cell dynamics and inflammation in obese adipose tissue. *Journal of Clinical Investigation*, *118*(2), 710–721.

Ohmura, K., Ishimori, N., Ohmura, Y., Tokuhara, S., Nozawa, A., Horii, S., et al. (2010). Natural killer T cells are involved in adipose tissues inflammation and glucose intolerance in diet-induced obese mice. *Arteriosclerosis, Thrombosis, and Vascular Biology*, *30*(2), 193–199.

Paddock, S. W., & Eliceiri, K. W. (2014). Laser scanning confocal microscopy: History, applications, and related optical sectioning techniques. *Methods in Molecular Biology*, *1075*, 9–47.

Rangel-Moreno, J., Moyron-Quiroz, J. E., Carragher, D. M., Kusser, K., Hartson, L., Moquin, A., et al. (2009). Omental milky spots develop in the absence of lymphoid tissue-inducer cells and support B and T cell responses to peritoneal antigens. *Immunity*, *30*(5), 731–743.

Spencer, M., Yao-Borengasser, A., Unal, R., Rasouli, N., Gurley, C. M., Zhu, B., et al. (2010). Adipose tissue macrophages in insulin-resistant subjects are associated with collagen VI and fibrosis and demonstrate alternative activation. *American Journal of Physiology: Endocrinology and Metabolism*, *299*(6), E1016–E1027.

Stockert, J. C., Villanueva, A., Cristóbal, J., & Cañete, M. (2009). Improving images of fluorescent cell labeling by background signal subtraction. *Biotechnic and Histochemistry*, *84*(2), 63–68.

Suzuki, M., Shinohara, Y., Ohsaki, Y., & Fujimoto, T. (2011). Lipid droplets: Size matters. *Journal of Electron Microscopy*, *60*(Suppl. 1), S101–S116.

Tabata, Y., Miyao, M., Inamoto, T., Ishii, T., Hirano, Y., Yamaoki, Y., et al. (2000). De novo formation of adipose tissue by controlled release of basic fibroblast growth factor. *Tissue Engineering (United States)*, *6*(3), 279–289.

Tsui, H., Wu, P., Davidson, M. G., Alonso, M. N., & Leong, H. X. (2011). B cells promote insulin resistance through modulation of T cells and production of pathogenic IgG antibodies. *Nature Medicine*, *17*(5), 610–617.

Xu, H. H., Barnes, G. T. G., Yang, Q. Q., Tan, G. G., Yang, D. D., Chou, C. J. C., et al. (2003). Chronic inflammation in fat plays a crucial role in the development of obesity-related insulin resistance. *Journal of Clinical Investigation*, *112*(12), 1821–1830.

Zuk, P. A. P., Zhu, M. M., Ashjian, P. P., De Ugarte, D. A. D., Huang, J. I. J., Mizuno, H. H., et al. (2002). Human adipose tissue is a source of multipotent stem cells. *Molecular Biology of the Cell*, *13*(12), 4279–4295.